LEGIBILITY NOTICE

A major purpose of the Technical Information Center is to provide the broadest dissemination possible of information contained in DOE's Research and Development Reports to business, industry, the academic community, and federal, state and local governments.

Although a small portion of this report is not reproducible, it is being made available to expedite the availability of information on the research discussed herein.

LA-UR--89-3397

DE90 002387

TITLE *INEX Simulations of the Los Alamos HIBAF Free-Electron Laser MOPA Experiment*

AUTHOR(S) *John C. Goldstein, Bruce E. Carlsten, and Brian D. McVey*

SUBMITTED TO *Proceedings of the 1989 FEL Conference to be published in Nucl. Instr. and Meth. in Phys. Res.*

DISCLAIMER

Los Alamos National Laboratory
Los Alamos, New Mexico 87545

INEX Simulations of the Los Alamos HIBAF Free-Electron Laser MOPA Experiment *

John C. Goldstein, Bruce E. Carlsten and Brian D. McVey
Group X-1, MS E531
Los Alamos National Laboratory
Los Alamos, NM 87545
(505) 667-4370
(505) 665-3389 (FAX)

ABSTRACT

We present results of Integrated Numerical Experiment (INEX) simulations of the performance of a 1-m untapered wiggler FEL oscillator driving a 2-m wiggler FEL amplifier for the new HIBAF (High-Brightness Accelerator Free-Electron Laser) facility at Los Alamos. INEX simulations utilize a numerically-generated electron micropulse, from ISIS/PARMELA calculations of the photoinjector/linac/beam transport system, in the 3-D FEL simulation code FELEX.

I. Introduction.

The Los Alamos free-electron laser facility has been substantially modified by the addition of a photocathode injector for the linac and two additional accelerator tanks. A very bright beam with an energy near 40 Mev will be generated. This will allow operation of FELs at an optical wavelength near 3 μm if already existing wigglers are used. The facility [1], which has been named HIBAF for High-Brightness Accelerator Free-Electron Laser, will contain two wiggler magnets which will be excited in series by the same electron beam. A new 150° bend magnet will transport electrons, which have traversed the 1-m wiggler of the Los Alamos FEL oscillator, into a variable gap 2-m wiggler, to be constructed and supplied by the Rocketdyne division of Rockwell, Inc. The 2-m wiggler will be used as a single-pass amplifier in FEL MOPA (Master Oscillator Power Amplifier) experiments. The calculated performance of FEL MOPA experiments is the subject of the present paper although many other FEL configurations (e.g., high power oscillator with a ring optical resonator) are being planned for future HIBAF experiments.

* Work performed under the auspices of the U.S. Department of Energy and supported by the U.S. Army Ballistic Missile Defense Organization.

Since the same electron beam will be used to excite both wigglers, the oscillator will have to be constrained to low power operation so that the electron beam quality (energy spread in this case) will be maintained for use in the amplifier. We will discuss several methods for such operation of the oscillator.

We distinguish two possible regimes for amplifier operation: in the limit of no energy spread added by the oscillator to the electron beam, very large (> 1000) small-signal gains are possible in the (untapered) amplifier; at higher oscillator power levels, with greater induced energy spread added to the electron beam, moderate gains (10-30) are possible (with the amplifier untapered or slightly tapered). Phenomena in both the high gain and the moderate gain regimes will be accessible to experimental study. We present calculated results for both regimes.

Extensive numerical simulations of the HIBAF photoinjector/linac/beam transport system have been done [2]. The numerically-generated electron micropulse from those calculations is used in the 3-D FEL simulation code FELEX [3, 4, 5] to quantitatively predict FEL performance. We have extended this INEX (Integrated Numerical Experiment) method by returning the electron beam to the accelerator code PARMELA after it has interacted with the optical field in the oscillator. The electrons are then numerically transported around the 150° bend magnet and focused into the Rocketdyne 2-m amplifier wiggler. The electrons are then again inserted into FELEX at that point to calculate the amplifier performance. The INEX method of coupled accelerator-FEL simulations has yielded results in good agreement with FEL oscillator experiments [6, 7].

Finally, we exhibit results of an INEX simulation of a high power oscillator which uses a 1 m parabolically tapered wiggler.

II. Description of HIBAF Facility.

A schematic layout of the principal components of the HIBAF facility is shown in Fig. 1. The 40 Mev linac consists of a photocathode preparation chamber and four accelerator tanks. An isochronous 60° bend magnet at the end of the accelerator guides the beam into

the 1-m oscillator wiggler. Following its interaction with the oscillator's optical field in the 1-m wiggler, the electron beam is transported to the 2-m amplifier wiggler by a new 150° bend magnet. Great care [2] has been taken in the design of the linac/beam transport system to minimize the deleterious effects of wakefields upon the electrons, particularly in the highly dispersive sections of the 60° and 150° magnets.

The optical resonator for the oscillator is designed for an optical wavelength of 3 μm. It will consist of two CaF_2 mirrors, of radii of curvature 3 and 4 meters, separated by about 6.93 m. Each mirror will have a reflectivity of about 99%. The lowest order Gaussian cavity mode has a Rayleigh range of 37 cm and is focused at the center of the wiggler. Relay optics will transport light from the oscillator to the amplifier, as shown in Fig. 1.

For MOPA experiments, the 1-m oscillator wiggler will be untapered and will have a peak wiggler field B_{w} of 3214 G and a wavelength λ_{w} of 2.73 cm (thus giving a dimensionless vector potential a_{w} of 0.8184). For high power oscillator experiments, a different 1-m wiggler will be used: it has a 30% taper (in $k_{w} = 2\pi/\lambda_{w}$).

The 2-m amplifier wiggler will be constructed and supplied by Rocketdyne. That device will have a fixed wavelength $\lambda_{w} = 2.4$ cm but will have a variable gap. With a full gap of about 1 cm, $B_{w} = 4548.7$G ($a_{w} = 1$) will be needed to produce gain at 3 μm with the 40 Mev HIBAF electron beam. This wiggler can be linearly tapered in B_{w} by opening up the gap at the exit end a little more than the gap at the entrance. More complicated tapers are not possible. Both the Rocketdyne wiggler and the various 1-m oscillator wigglers are flat pole face devices which produce a linearly polarized wiggler field. Further details of the features of the Rocketdyne wiggler can be found in [8].

III. Amplifier Performance Determines Constraints On Oscillator Performance.

A MOPA FEL in which electrons from one accelerator drive both the oscillator and the amplifier is sometimes referred to as a SAMOPA (Single Accelerator MOPA). In the HIBAF SAMOPA FEL, electrons will traverse the oscillator and the amplifier wigglers consecutively. The energy spread of the electron beam will be increased as a result of its

interaction with light in the oscillator. The higher the operating power of the oscillator, the larger will be the energy spread induced in the electron beam. The performance of the amplifier decreases with increasing electron beam energy spread; hence, the oscillator must run weakly so as not to increase too much the energy spread of the electrons which are sent on to the amplifier. On the other hand, the performance of a tapered wiggler amplifier increases with increasing input optical power. Therefore, the design of the HIBAF SAMOPA system needs to provide for an oscillator which can maintain the brightness of the electron beam at an acceptable level and still provide sufficient light to drive the amplifier to desired levels.

It should be noted that other SAMOPA designs may utilize electron beam and optical beam switching techniques that can circumvent this problem [9]. Also, a SAMOPA design in which the electron beam traverses the amplifier first has been proposed [10]. The HIBAF SAMOPA must also satisfy constraints of available laboratory space, available equipment, and program schedule requirements. Thus, some of the other possible design schemes for a SAMOPA FEL system were not considered for HIBAF.

One can envisage at least two different HIBAF SAMOPA operating regimes: (1) An untapered amplifier with a very low power oscillator. Under these conditions, a very large (> 3000) small-signal gain has been calculated using a PARMELA-generated electron micropulse. High gain FEL physics at an optical wavelength of 3 μm can be studied in this configuration. (2) A linearly tapered amplifier wiggler and a moderate power oscillator: this would be used for maximum power and extraction efficiency from the SAMOPA FEL system.

In order to determine approximately the allowable oscillator induced energy spreads for these two cases, we calculated the dependence of the amplifier performance upon electron beam rms energy spread using a model electron beam with approximately the same characteristics as expected to occur in the full PARMELA accelerator simulation: peak micropulse current I = 250 A, normalized "90%" emittance $\epsilon_n = 50\pi$ mm - mr, and frac-

tional energy spread $\Delta\gamma/\gamma = 0.25\%$. For the 2-m Rocketdyne wiggler in an untapered configuration, the small-signal gain dropped by about a factor of two for an increase by a factor of two (from 0.25% to 0.5%) in rms energy spread. For this wiggler in a linearly tapered configuration with a 6% total taper in B_w, with 9.2 MW optical input, the amplifier's gain and extraction efficiency dropped by about a factor of two when the electron beam rms energy spread increased by about a factor of four (from 0.25% to 1.0%).

Hence, we conclude that the oscillator must be operated so as to increase the original electron beam energy spread by factors of about 2 to 6 (up to 0.5% to 1.5%). Note that these estimates neglect the change in shape of the energy distribution that accompanies an increase in the rms energy spread. That is, the effect on the amplifier of increasing the rms energy spread by a factor of four will differ for distributions of different shapes having the same rms spread. However, the approximate range of acceptable induced energy spread increases is known.

IV. Controlling the Oscillator Power Level.

The calculated maximum (with respect to optical wavelength) small-signal gain of the oscillator with the untapered wigger of Sec. II is about 550%. Since the cavity losses are expected to be only about 2%, this device will saturate at a very high optical intensity and induce an unacceptably large energy spread on the electron beam. The oscillator can be operated at low power by (1) reducing the small-signal gain and (2) increasing the optical resonator losses. The gain can be reduced by (a) defocusing the electron beam in the wiggler, (b) using a Littrow grating (or other wavelength filter) to tune the laser wavelength over the gain curve, and (c) adjusting the length of the optical resonator for laser operation on the wing of the length detuning (desynchronism) curve. The cavity losses can be increased by adjusting the electron beam energy so that the resonant wavelength falls in the lower reflectivity (higher transmission) region of the dielectric mirrors. Evidently, a combination of all of these techniques can be used simultaneously to produce stable oscillator operation at low power.

Since the saturated power level (in the absence of sidebands) in a uniform wiggler FEL oscillator varies approximately as N^{-4}, where N is the number of periods of the wiggler field, one might think of limiting the oscillator power level by using a very long wiggler. In the case of HIBAF, a wiggler longer than 1-m would not fit into the available space along the electron beamline. Hence, this option - which also would require the construction of an entirely new wiggler - was not seriously considered.

Since the maximum gain of the oscillator is so large, methods (b) and (c) for gain reduction suffer from the difficulty of reducing the gain close to, but still above, zero. That is, for cavity losses of 2%, the gain would have to be reduced from 550% to perhaps 5% to keep the oscillator power level low. Such a large reduction, by wavelength tuning or cavity length tuning, is possible in principle, but would be hard to achieve experimentally since small fluctuations in the micropulse current — which will probably exist — can momentarily shut off the laser. In order to avoid sensitivity to such fluctuations, a method of gain reduction originally proposed by W. Stein [11] has been studied and appears to be quite promising.

The method proposed by Stein is to reduce the gain by increasing the size of the electron beam in the oscillator wiggler. Since the wiggler is a planar wiggler, the usual focusing of the electrons involves matching the beam size in the plane of the betatron motion, according to the emittance and the wiggler field; the "natural focusing" of the wiggler keeps this dimension constant during traversal of the wiggler [12]. In the other ("wiggle") plane, the electrons are externally focused such that the beam size at the center of the wiggler, $\tilde{x}$, is equal to the matched beam size in the betatron plane, $\tilde{y}$. Stein's suggestion is to defocus the beam in the x-direction such that $\tilde{x} = n\tilde{y}$, where n is an integer in the range 2 10. Figure 2 shows a plot of the radius of the vacuum lowest order optical mode of the HIBAF cavity as a function of position in the 1-m uniform wiggler. The electron-beam radius in the y-direction is the solid line (constant value about 0.041 cm). The curves labeled n=1, n=2, n=4, and n=8 show the electron beam x-radius versus

position in the wiggler for various amounts of defocus. Increasing the beam size in the x-direction reduces the interaction with the optical mode and so reduces the gain.

Figures 3–6 show calculated oscillator performance data for electron beam focusing characterized by n=1, 2, 4, and 8 respectively. Each figure consists of a pair of graphs: the left-hand graph shows gain vs. optical wavelength, with optical power as the parameter that distinguishes different curves; the right-hand graph shows the factor by which the rms energy spread of the electron beam has increased over its initial value vs. optical wavelength, with internal optical power again labeling different curves. These calculations were single-pass single wavefront calculations using the electron beam parameters of Sec. III.

The meaning of these calculations is this: Fig. 5, for example, shows that defocusing the electron beam to the n=4 condition produces gain curves whose maximum values are in the 60% - 80% range for intracavity powers of zero to 16 MW. In particular, at 8 MW and an optical wavelength of 2.86 μm, the gain is about 70%; if the reflectivity of each cavity mirror is 77% and there are no other losses, then the cavity loss would equal the gain at a steady-state internal peak power of 8MW. The right-hand graph of Fig. 5 shows that, at 2.86 μm and 8MW, the electron beam rms energy spread would be increased by about a factor of 2.5, which is in the desired range.

Thus, by defining the laser wavelength (by means of a Littrow grating or other intracavity wavelength filter) and the total cavity loss, one can fix the steady-state internal operating power of the oscillator and, therefore, the associated increase in energy spread added to the electron beam. Note that steady-state laser operation is possible only for wavelengths for which the small signal gain exceeds zero: that is for wavelengths greater than about 2.82 μm in Figs. 3-6. Note also that, for the curves shown in the right-hand graphs of Figs. 3-6, the cavity losses are varied as the laser wavelength varies: an easier mode of operation is to fix the cavity loss and vary the filter wavelength. This would lead to various steady-state power levels, with various associated induced energy spreads. We have chosen to present possible oscillator operating conditions as functions of slightly

different parameters.

V. INEX Results For n=4 Oscillator.

Figure 7 shows plots of the current, normalized emittances in the x (wiggle plane) and y (betatron plane) directions, and energy distribution of an electron micropulse from the accelerator simulations. This pulse was propagated through the linac/beam transport system up to the entrance to the 1-m oscillator wiggler and focused in approximately the n=4 configuration. Figure 8 shows the results of a 3-D finite pulse FEL calculation in which that electron micropulse was used on each pass of a multipass oscillator simulation using the FELEX code. The maximum calculated small signal gain was 84%, while each cavity mirror was assumed to have a reflectivity of .79 (37.6% round trip cavity loss). The oscillator saturates in about 150 passes with an optical pulse of about 40 MW peak power. Note the change of ordinate scales between the plots of the initial and final electron energy distributions.

The final electron distribution was then returned to PARMELA. That beam was propagated around the 150° bend magnet and focused into the 2-m Rocketdyne wiggler. Figure 9 shows the change in emittance caused by propagation around the bend magnet. The y emittance was not changed, but the x emittance (in the plane of the bend) was increased from about 25 π mm-mr to 33 π mm-mr at the center of the micropulse. The current and energy spread of the micropulse did not change during this stage of propagation.

The results of using the above micropulse in the 2-m Rocketdyne amplifier are as follows: with the amplifier in an untapered configuration, and light at the wavelength of oscillator operation, 2.9925 μm, a small-signal gain of 351.4 was achieved. This is substantially below the value of 3000 found with the electron micropulse before interaction in the oscillator and propagation around the 150° bend, but it does show that the high gain regime can be accessed by the HIBAF MOPA experiment.

If the Rocketdyne wiggler is configured with a 6% taper in B_w, the optical wavelength

is again 2.9925 μm, and we assume that the oscillator mirrors are such that 20% of the peak intracavity power, which amounts to 8 MW, can be delivered by the relay optics to the entrance of the amplifier, we find the results given in Table 1: by varying the gap to tune B_w in the amplifier, we obtained a maximum optical gain of about 16 and a maximum micropulse–averaged extraction efficiency of 0.66%. One could achieve a lot more in this mode of amplifier operation if the wiggler were not restricted to linear tapers, or if the wiggler were longer than 2 meters.

VI. INEX Results For A High Power Oscillator.

We have calculated the performance of an oscillator with the same optical cavity as used above and with a 1-m parabolically tapered wiggler instead of the uniform wiggler. With the numerically-generated micropulse focused into the wiggler for maximum gain, the results are shown in Fig. 10: a micropulse-averaged extraction efficiency of about 4% is reached with a peak intracavity optical power of about 20GW. We note that this fully 3-D finite pulse simulation did not have enough resolution to allow sidebands to grow, so the result must be understood to be valid in the presence of some type of optical filtering which would not allow the growth of sidebands.

VII. Summary and Conclusions.

A new FEL facility named HIBAF is being built at Los Alamos. Among the various kinds of experiments planned are SAMOPA studies with a low power oscillator and a 2-m amplifier wiggler to be supplied by Rocketdyne. High power oscillator experiments will also be done; all FEL experiments using existing wigglers will be done at a fundamental optical wavelength near 3 μm.

We have studied various methods of operating the oscillator at low power so as not to unduly perturb the electron beam which is sent on to drive the amplifier. Defocusing the electrons in the oscillator's wiggler looks quite feasible, but experimentally this idea will probably be combined with single wavelength operation using a Littrow grating and cavity length tuning. We have studied the performance of the MOPA system with INEX, and

have extended INEX to include repeated exchanges of electron micropulses between the accelerator simulation code PARMELA and the FEL simulation code FELEX. A specific configuration of defocused electron beam in the oscillator wiggler, combined with high-loss mirrors (this can easily be achieved by tuning the electron beam energy such that the laser wavelength falls on the rising transmission part of the dielectric mirror reflectivity curve), produced an internal power of 40MW with a modest increase of electron beam energy spread. Propagation of that electron beam through the 150° bend magnet increased the emittance by about 20%. The resulting beam produced a maximum gain of 350 with a small optical signal injected into an untapered amplifier; a gain of 16 and an extraction efficiency of 0.66% was achieved with a 6% taper in B_w and 8 MW peak power injected.

We have shown that both high gain and high extraction efficiency MOPA experiments are possible, and that the INEX method can be used to design and analyze such experiments. Hence HIBAF should be able to significantly extend the Stanford-Rocketdyne FEL MOPA experiments that were reported in [13]. With the very bright electron beam from HIBAF, we predict that a high power oscillator could reach peak optical powers of 20 GW inside the cavity and an extraction efficiency of 4% with a 1-m parabolically tapered wiggler.

Figure captions:

Figure 1: Schematic layout of HIBAF facility.

Figure 2: Optical and electron beam radii vs. position within the oscillator wiggler.

Figure 3: Calculated oscillator performance data for n=1.

Figure 4: Calculated oscillator performance data for n=2.

Figure 5: Calculated oscillator performance data for n=4.

Figure 6: Calculated oscillator performance data for n=8.

Figure 7: Electron micropulse properties at entrance to oscillator wiggler.

Figure 8: Calculated oscillator performance properties.

Figure 9: Emittance growth by propagation through the 150° bend magnet.

Figure 10: High power oscillator results.

References

1. "The Los Alamos High Brightness Accelerator FEL (HIBAF) Facility," W. Cornelius, S. Bender, K. Meier, L. E. Thode, J. M. Watson, these proceedings.
2. "Accelerator Design and Calculated Performance of the Los Alamos HIBAF Facility," B. E. Carlsten, L. M. Young, M. E. Jones, B. Blind, E. M. Svaton, K. C. D. Chan, and L. E. Thode, these proceedings.
3. "Three-Dimensional Simulations of Free-Electron Laser Physics," B. D. McVey, Nucl. Instr. and Meth. in Phys. Res. A250, pp. 449-455 (1986).
4. "Numerical Simulations of Free-Electron Laser Oscillators," B. D. McVey, J. C. Goldstein, R. L. Tokar, C. J. Elliott, S. J. Gitomer, M. J. Schmitt, and L. E. Thode, to be published in Nucl. Instr. and Meth. in Phys. Res. in the proceedings of the 1988 FEL Conference.
5. "Simulation Codes for Modeling Free-Electron Laser Oscillators," J. C. Goldstein, B. D. McVey, R. L. Tokar, C. J. Elliott, M. J. Schmitt, B. E. Carlsten, and L. E. Thode in *Modeling and Simulation of Laser Systems*, Donald L. Bullock, Editor, Proc. SPIE 1045, pp. 28-35 (1989).
6. "Integrated Numerical Modeling of Free-Electron Laser Oscillators," J. C. Goldstein, B. D. McVey, B. E. Carlsten, and L. E. Thode, to be published in Nucl. Instr. and Meth. in Phys. Res. in the proceedings of the 1988 FEL Conference.
7. "INEX Simulations of the Boeing FEL System," R. L. Tokar, L. M. Young, A. H. Lumpkin, B. D. McVey, L. E. Thode, S. C. Bender, K. C. D. Chan, A. D. Yeremian, D. H. Dowell, and A. R. Lowrey, these proceedings.
8. "High Performance Pure Permanent Magnet Undulators," G. Rakowsky, B. Bobbs, W. McMullin, G. Swoyer, these proceedings.
9. "Design Concept for a Common RF Accelerator Driven Free Electron Laser Master Oscillator/Power Amplifier," A. Bhowmik, J. M. J. Madey, and S. V. Benson, Nucl.

Instr. and Meth. in Phys. Res. A272, pp. 183-186 (1988).

10. B. E. Newnam, private communication, June, 1985.
11. W. Stein, private communication, December, 1988.
12. "Gain Physics of RF-Linac-Driven XUV Free-Electron Lasers," J. C. Goldstein, B. D. McVey, and B. E. Newnam in *Short Wavelength Coherent Radiation: Generation and Applications*, AIP Conference Proceedings No. 147, D. T. Attwood and J. Bokor Eds. (American Institute of Physics, 1986), pp. 275-290.
13. "Initial Results from the Free-Electron Laser Master Oscillator/Power Amplifier Experiment," A. Bhowmik, M. S. Curtin, W. A. McMullin, S. V Benson, J. M. J. Madey, B. A. Richman, and L. Vintro, these proceedings.

Table 1: Gain and extraction efficiency of 2-m amplifier wiggler with a 6% B_w taper as a function of initial magnetic field for an incident power of 8 MW.

B_w (initial), G	Optical Gain	Pulse-averaged extraction efficiency, %
4594.229	8.321	0.3174
4639.716	13.75	0.5528
4662.460	15.43	0.6253
4685.204	16.25	0.6606
4730.691	15.69	0.6361

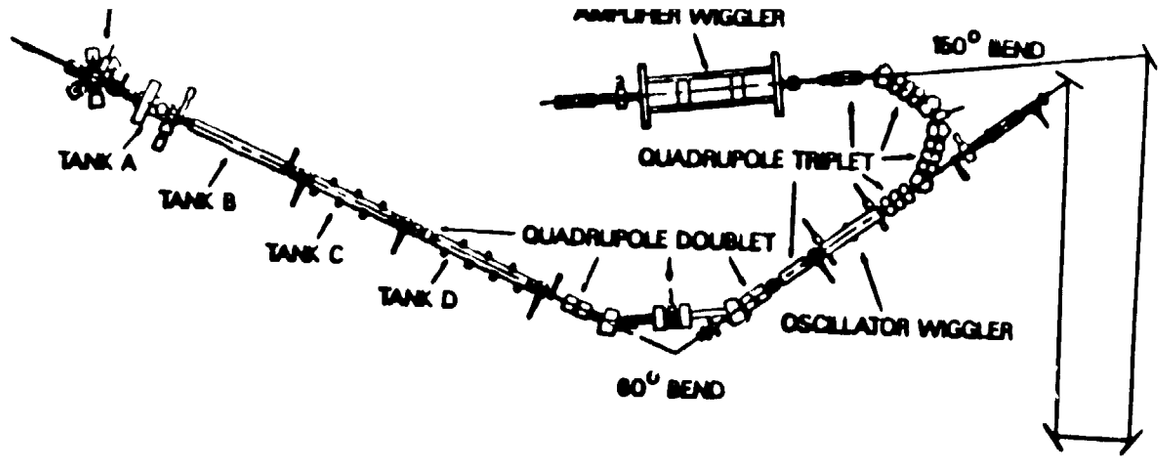

Figure 1

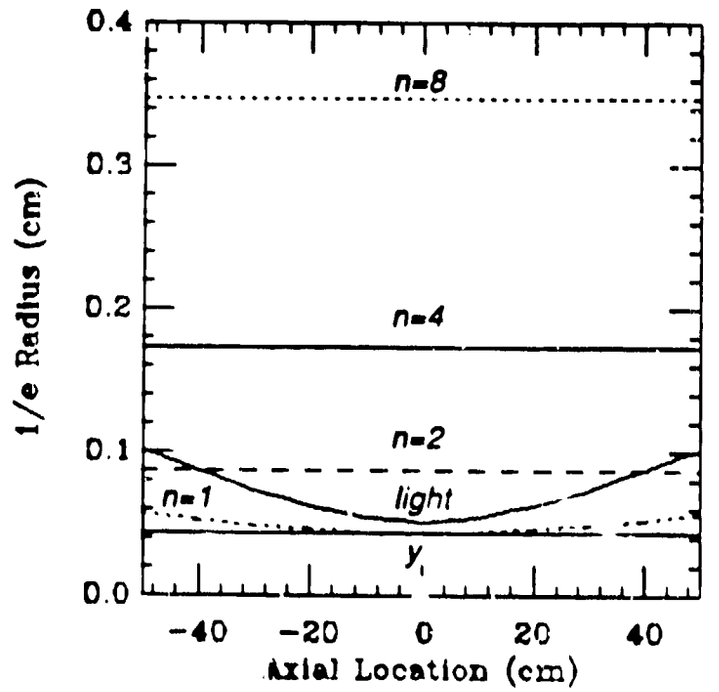

Figure 2

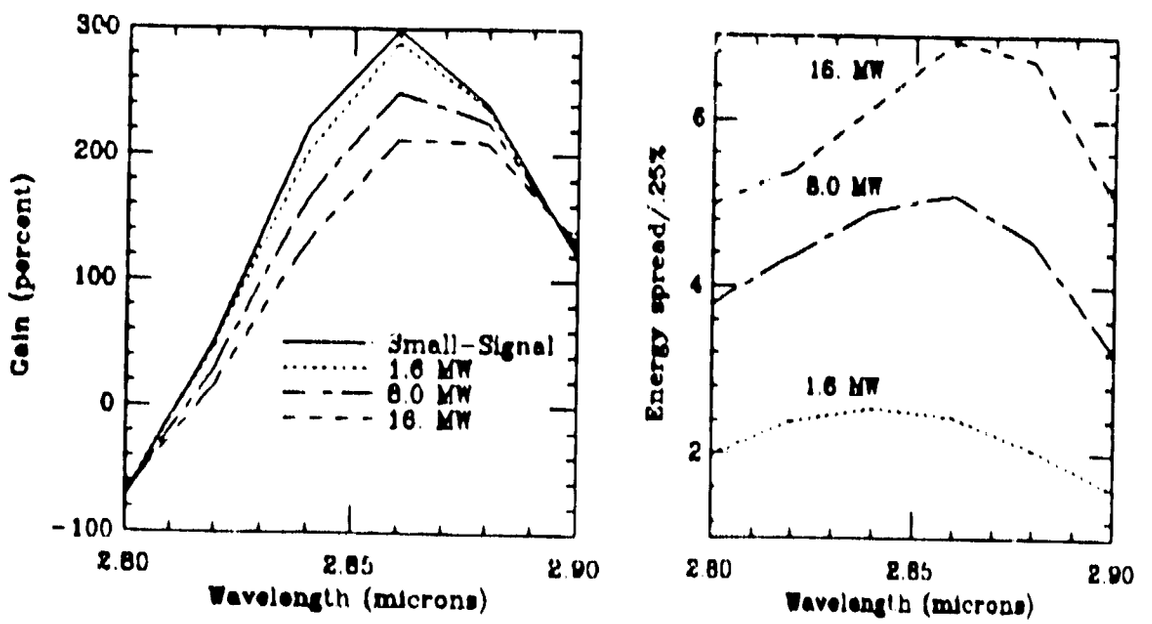

Figure 3

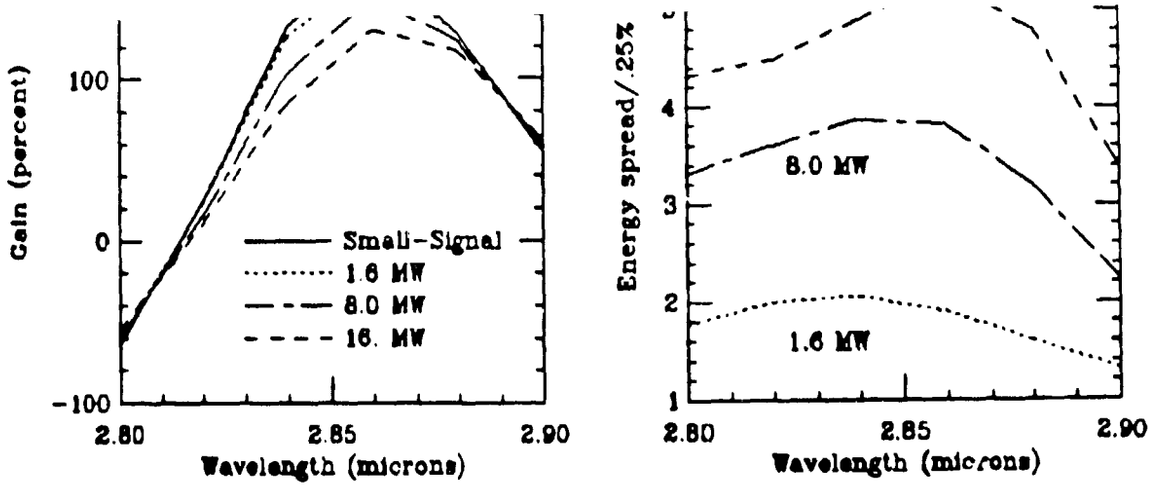

Figure 4

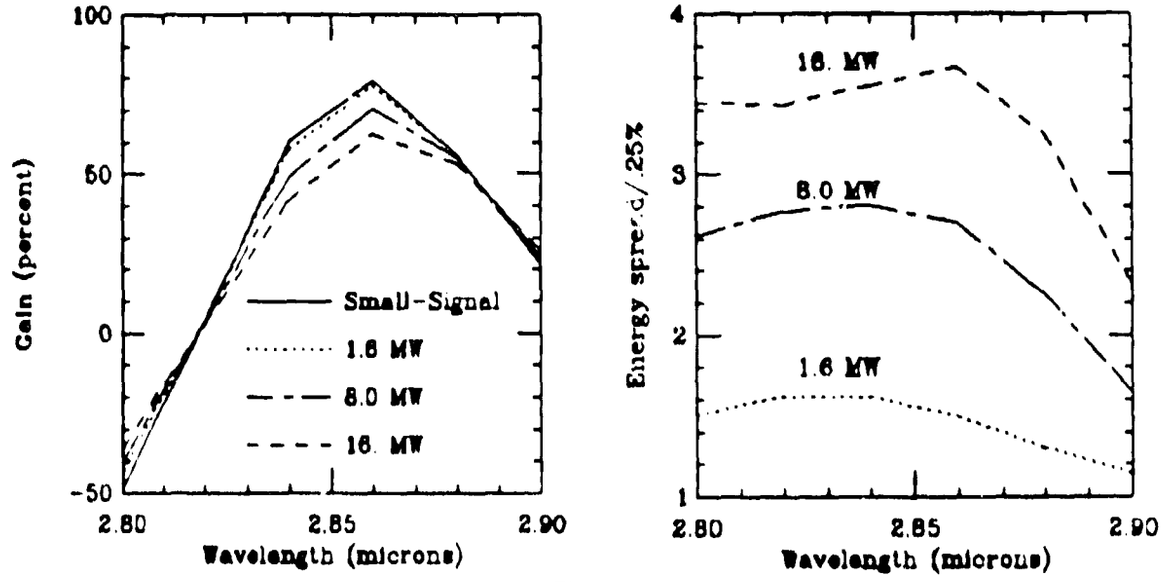

Figure 5

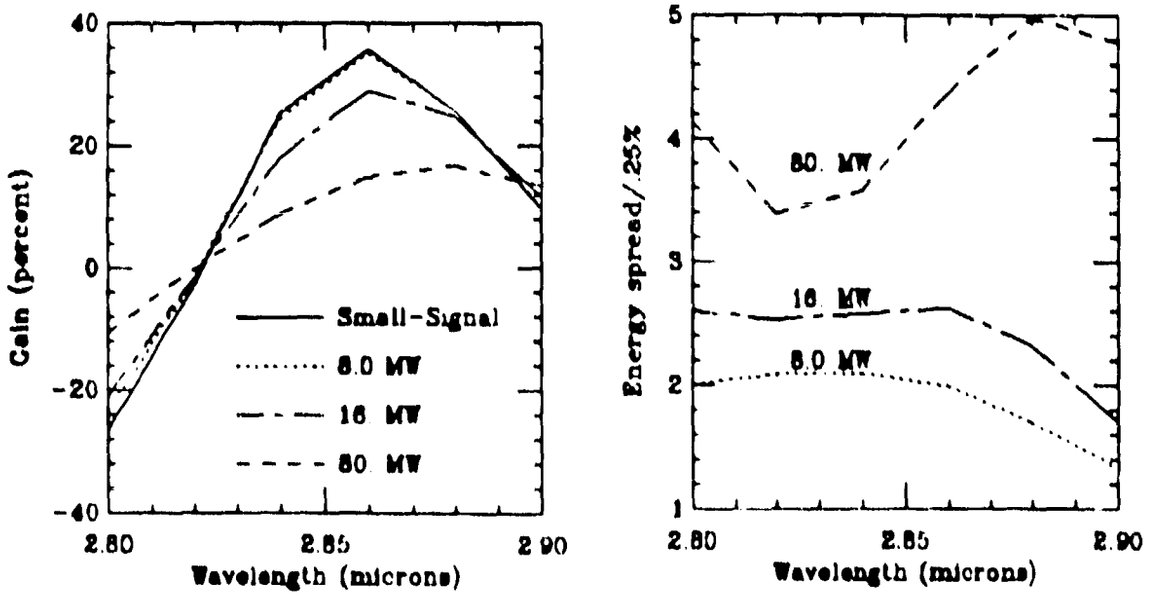

Figure 6

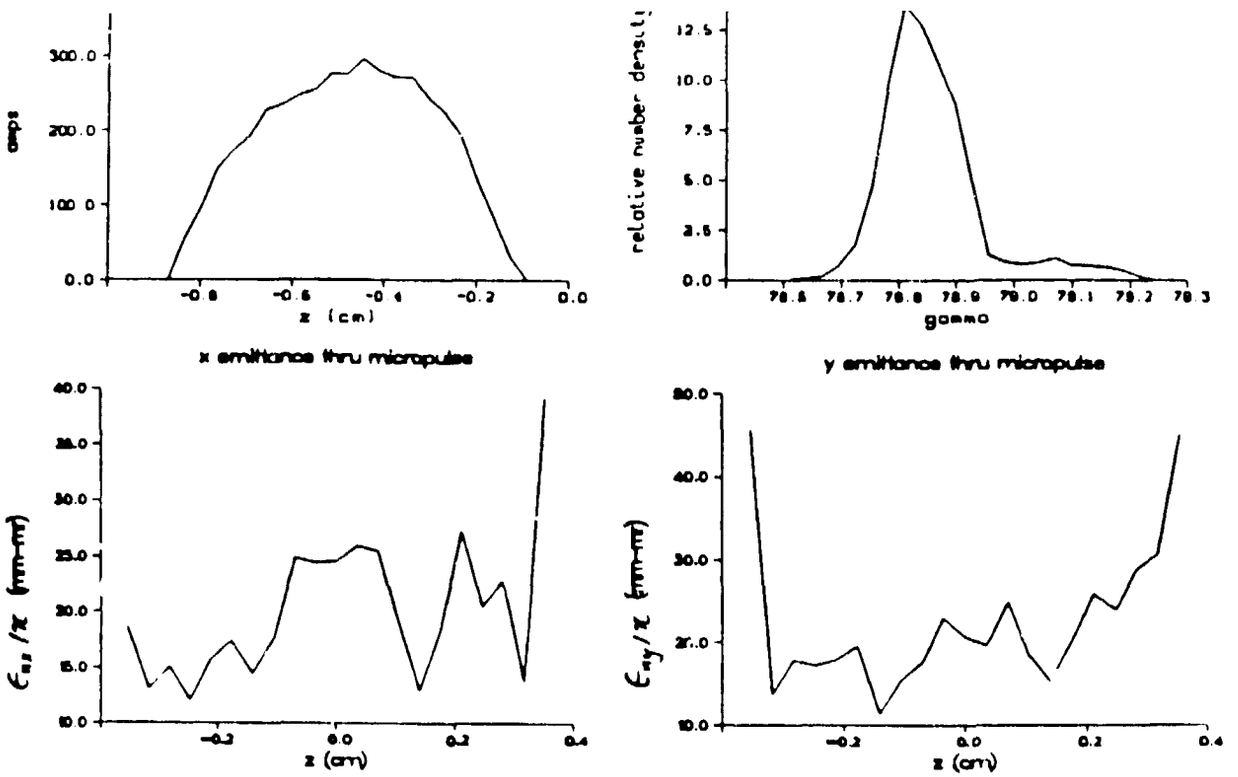

Figure 7

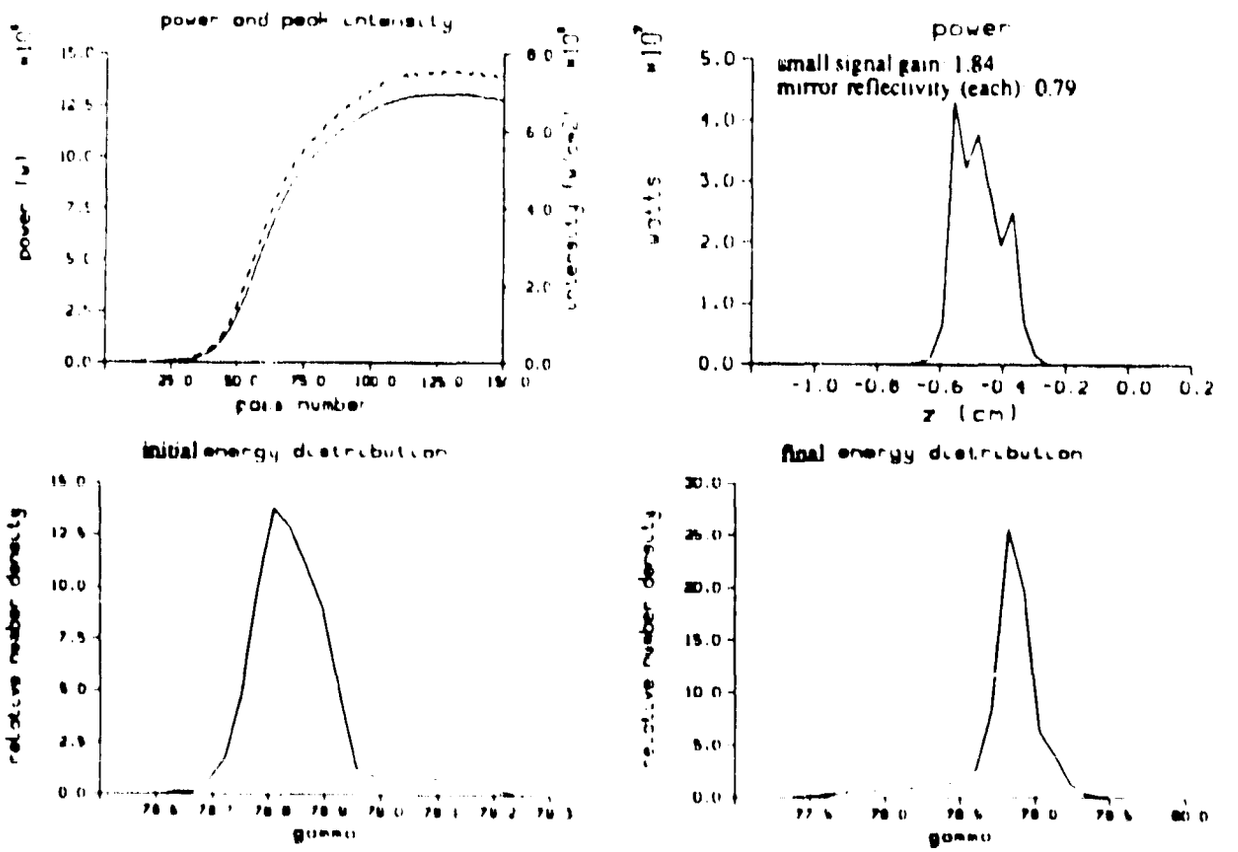

Figure 8

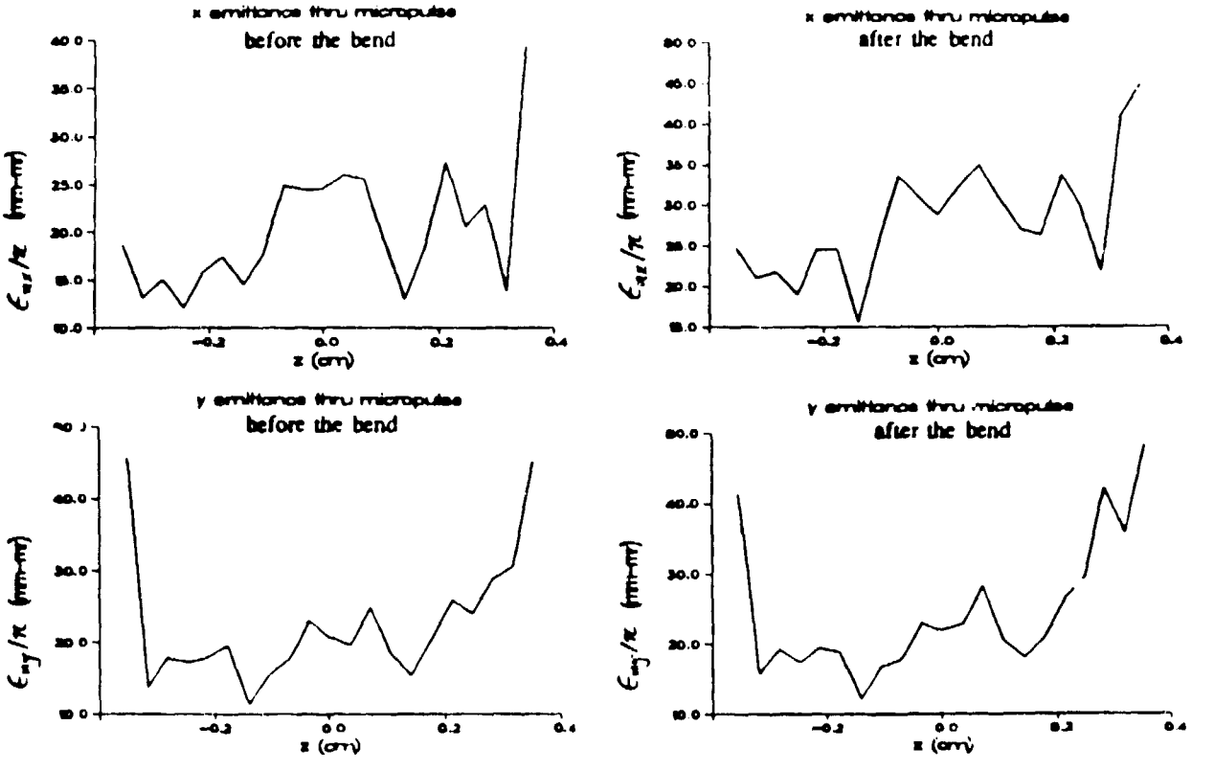

Figure 9

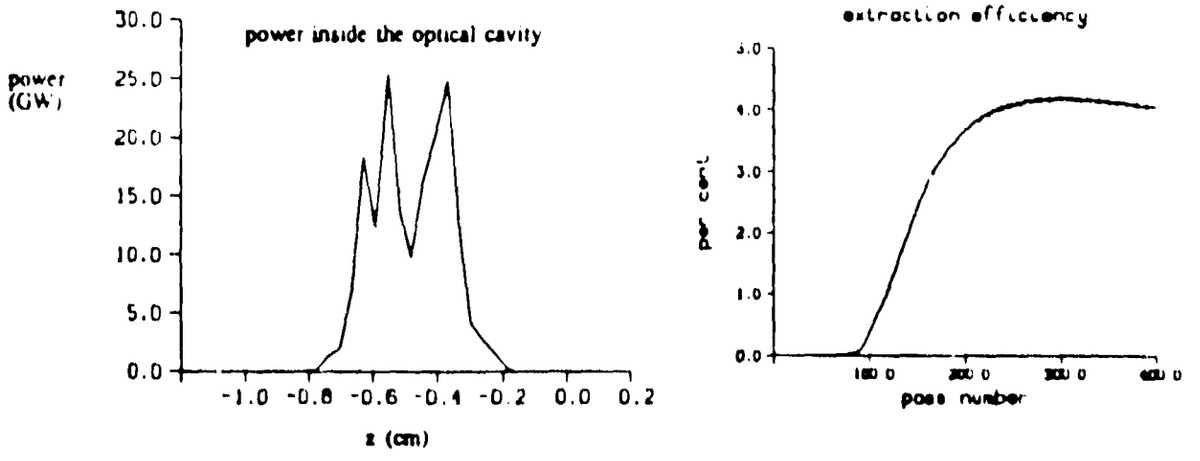

Figure 10